International Journal of Microwave and Wireless Technologies, 2011, 3(6), 691–699.
doi:10.1017/S1759078711000985

RESEARCH PAPER

Genetic algorithm for optimization of L-shaped PIFA antennas

TRONG DUC NGUYEN[1], YVAN DUROC[2], VAN YEM VU[3] AND TAN PHU VUONG[1]

Two new designs of the L-shaped Planar Inverted–F Antenna (PIFA) antennas with single and dual polarization operating at the frequency band for IEEE 802.11b/g standard with satisfactory radiation characteristics are presented. We further propose a genetic algorithm (GA) embedded in CST Microwave Studio for optimizing these antenna parameters. The agreement of simulation and measurement results shows the performance of our joint model. Also, they show that our dual-polarization antenna is suitable for indoor Multiple Input Multiple Output (MIMO) wireless environment applications.

Keywords: Genetic algorithm, Optimization, L-shape PIFA antenna, Population

Received 31 March 2011; Revised 9 September 2011

I. INTRODUCTION

Nowadays, the development of mobile communication and the miniaturization of radio frequency transceivers are experiencing an exponential growth, hence increasing the need for compact antennas. As a result, new antenna prototypes have been developed to provide a larger bandwidth as well as a small dimension. The PIFA antenna is one of the most potential models.

The PIFA antenna has found widespread internal utilization within wireless terminals, thanks to its compact size for both single- and dual-band applications as well as single and dual polarizations. The PIFA antenna has several advantages such as the ease of fabrication, low implementation cost, a compatibility and conformity of ground plane with complex geometries [1, 2]. However, in this antenna, the length of microstrip patch, the thickness of the air layer between the patch and the ground plane as well as the shorting pin position strongly influence the antenna reflection coefficient and operating frequency [3, 4]. It is difficult to have operating frequency with an optimal antenna input reflection coefficient in each frequency band. Therefore, antenna parameter optimization is a critical issue. Many algorithms have been developed for this purpose, one of which is genetic algorithm (GA) [5, 6]. GA is a stochastic searching algorithm that acts on a population of possible solutions. They are based on the mechanisms of population genetics and selection [5]. A lot of applications used GA to optimize the parameters of antenna. In [7], a GA is used to design and optimize a monopole antenna by selecting the best configuration of the antenna when the length of the monopole changes. In [8], a combination of GA and Finite Difference Time Domain (FDTD) based on cost function is used to optimize the antenna's structure and loading conditions for maximal main lobe gain in a single azimuth direction. In [8], a GA is used to adaptively alter the polarization and directivity of a crossed dipole antenna.

In this paper, two new designs of the L-shape PIFA antennas with single and dual polarization are proposed. These two antennas operate at the frequency band for IEEE 802.11b/g standard with satisfactory radiation characteristics. The simulation and measurement parameters achieved show that our proposed dual-polarization antenna is suitable for indoor MIMO wireless environment applications. A specific GA auto-embedded in CST Microwave Studio software has been developed to optimize the proposed designs in terms of performance and dimension. This paper presents several relevant novelties in comparison with our recent work [9]. In particular, more parameters of the antenna are optimized and the simulations are carried out on much more individuals. In Section II, we first describe the structure of the designed antennas and then present how to use GA for optimizing our antennas. In Sections III and IV, the two PIFA antennas are, respectively, detailed with respect to the design, simulation, optimization and measurement. Conclusions are finally given in Section V.

II. L-SHAPED PIFA ANTENNA AND OPTIMIZATION PROBLEM

A) PIFA antenna

The Inverted-F Antenna (IFA) typically consists of an element radiation plate located above a ground plane, a short circuit or shorting pin and a feeding mechanism for element radiation [1, 10]. IFA is a variant of the monopole antenna in which the first part of the monopole is folded parallel to the ground plane in

[1] Laboratory IMEP-LAHC, Grenoble INP, 3 Parvis Louis Neél BP 257.38016, Grenoble, Cedex 1, France.
[2] Laboratory LCIS, Grenoble INP, 50 Barthélémy de Laffemas BP 54 26902, Valence, Cedex 9, France.
[3] School of Electronics and Telecommunications, Hanoi University of Science and Technology, 1 Dai Co Viet Road, Hanoi, Vietnam.
Corresponding author:
T. D. Nguyen
Email: Trong-Duc.Nguyen@minatec.inpg.fr

order to reduce the height of the antenna, while the resonance is still maintained. With this type of antenna, the ground plane plays a major role in the operation of the antenna. The current on the ground plane is bent by the excitation of the current on the surface of the radiation patch and the resulting electromagnetic field is formed by the interaction of the IFA and an image of itself below the ground plane. The capacitance and the input impedance of the antenna are replaced by a shorting pin that connects between the radiation elements to the ground plane. IFA is able to receive both vertically and horizontally polarized electromagnetic waves.

PIFA is considered to be a kind of linear IFA in which the radiation element is replaced by a radiation patch in order to expand the bandwidth as well as minimize the power of electromagnetic wave and reduce its absorption. PIFA is suitable for indoor wireless environment since it is of high-gain in both vertical and horizontal states of polarization. Figure 1 shows the geometry of a PIFA antenna.

B) L-shaped PIFA antenna

The L-shaped microstrip patch is illustrated in Fig. 2. The antenna is fed through a discrete port on the ground plane. The shorting pin connects the microstrip patch to the ground plane mounted on a dielectric substrate.

The radiation patch length of an L-shape PIFA antenna is easily varied. Therefore, the reflection coefficient and operating frequency of antenna are both easily turned variable without changing antenna size. Thus, the antenna can be minimized as well as the space can be saved.

C) Optimization of the L-shaped PIFA antenna by using GA

The application of GA to antenna parameter optimizations is not novel. The recent versions of CST Microwave Studio have their own embedded GA [11]. However, optimizing antenna parameters can only be done with the tools of the CST software. Consequently, users are restricted by only available CST tools. Using our method, the users can optimize the antenna parameters in such a way they need and they can use their own data format for example. In other words, the proposed method allows being independent of the CST tools. This approach also allows the GA algorithm to be embedded in other simulation softwares.

In this application, we use GA to optimize multiple simultaneously parameters of the antenna in order to simplify the procedure (the principle and activity of GA for PIFA antenna optimization will be detailed further below). The GA is embedded in the CST tool Macro. Thus, the construction, simulation, and optimization of the antenna can be fully implemented through the available functions of CST and programming language Visual Studio in file*. BAS (the interface and example of source codes are shown in Fig. 3). The FDTD method is used to calculate electromagnetic characteristics of antennas.

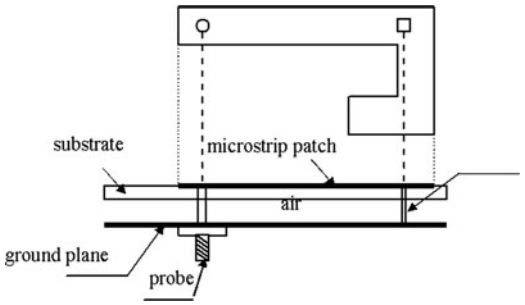

Fig. 2. Architecture of PIFA antenna L-shape.

The most important factor in the GA algorithm is the selection of individuals and fitness function.

For the PIFA antenna structures presented previously, as illustrated in Fig. 1, the resonant frequency f_r is calculated using the following formulas [1, 3].

$$f_r = \begin{cases} rf_1 + (1-r)f_2 & \text{if } w/l \le 1 \quad (1) \\ r^m f_1 + (1-r^m)f_2 & \text{if } w/l > 1 \quad (2) \end{cases}$$

where

$$f_1 = \frac{c}{4(l+h)} \tag{3}$$

$$f_2 = \frac{c}{4(l+w+h-s)} \tag{4}$$

$$r = \frac{s}{w} \tag{5}$$

$$m = \frac{w}{l} \tag{6}$$

where c is the speed of light, s is the width or radius of the shorting pin, l and w are the length and width of the microstrip patch, respectively, h is the thickness of the air layer between the patch and the ground plane.

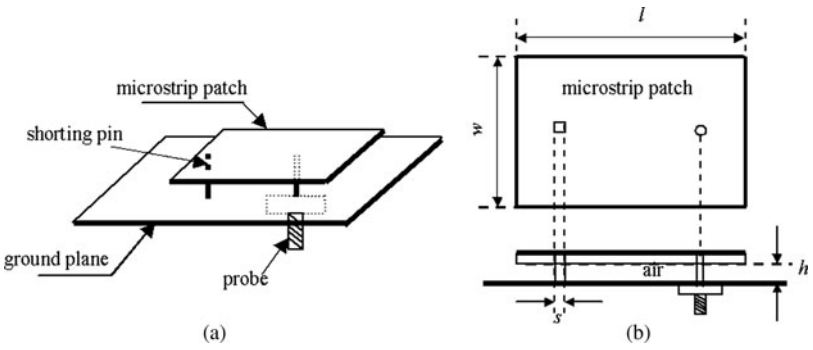

Fig. 1. Geometry and parameters of PIFA antenna.

https://doi.org/10.1017/S1759078711000985 Published online by Cambridge University Press

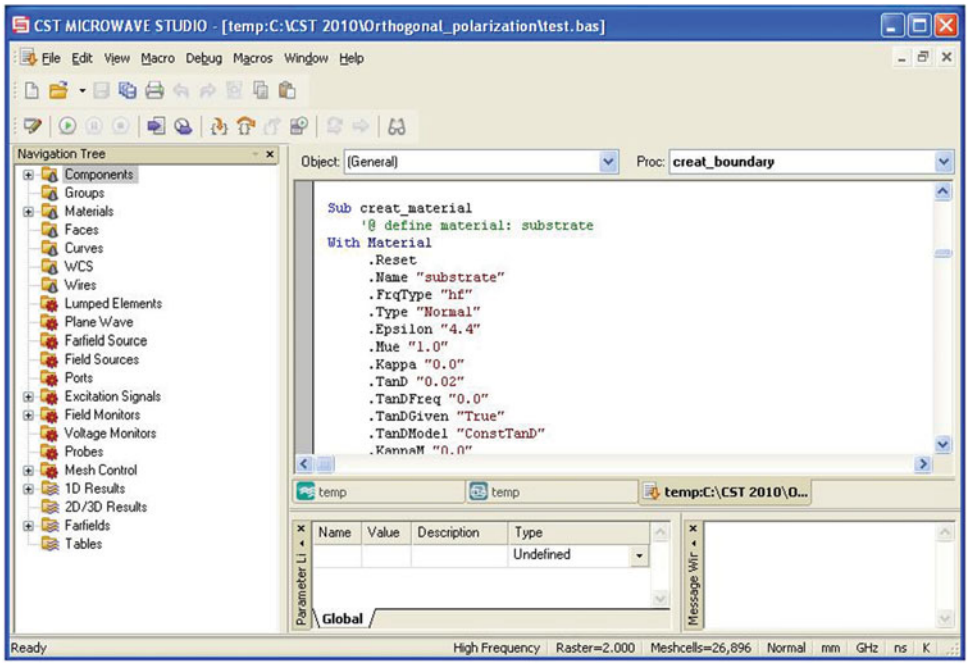

Fig. 3. The interfaces and example of source code in CST Macro.

These antennas operate in the frequency band ranging from 2.41 to 2.47 GHz. The dielectric substrate proposed is FR4 with thickness of 1.6 mm (a relative permittivity of 4.4 and a loss tangent of 0.02). Then by applying equations (1), (3), (4) and (6), we obtain the dimensions of antenna: $l = w \approx 40$ mm.

To optimize this antenna, we used the following individuals: the length of microstrip is represented by a 13-bit binary string (the maximum length of the antenna's patch is 40 mm); the thickness of the air layer between the patch and ground plane is represented by a 10-bit binary string; the discrete position and shorting pin position are represented by the 13-bit binary string.

The number of individuals used to optimize the antenna is 4 and each individual is encoded by the binary string with minimum length of 10. Therefore, the number of calculations done in the optimization process is very large and the memory can be overload. To avoid huge calculations and memory overload, we performed the GA algorithm on antennas with only two or three variable parameters. In addition, for simplify, the value of the binary the string bit encoding these populations is converted and displayed in decimal form.

As a requirement, the frequency band must be between 2.41 and 2.47 GHz. Otherwise, the fitness functions are selected as follows:

(1) For adaptation of antenna: fitness = min ($S_{11} < -15$ dB).
(2) For coupling between two antennas: fitness = ($S_{12} < -15$ dB).

In the case of single polarization antenna, only the first function is considered. In the case of dual polarization, both the functions are taken into account to traduce the effect of one resonant element on the other (i.e. isolation characteristic). Detailed forms of the final fitness function for each antenna are described in the below Step 3.

The principle of GA for optimization of PIFA antennas is shown in Fig. 4.

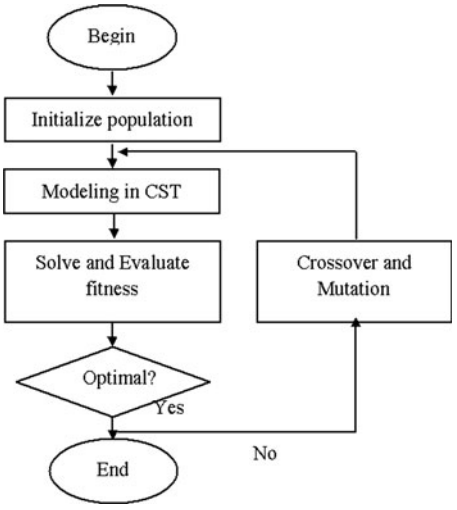

Fig. 4. Principle of GA for optimization of PIFA antennas.

GA's activity consists of:

Step 1: Initializing a population. There are six components: ground plane, substrate, air, microstrip patch, discrete port and shorting pin. Random generation of initial population includes the length of microstrip, the thickness of the air layer, the position of discrete port and the position of shorting pin.

Step 2: Creating the antenna and solving the model in CST software. In this step, the frequency and the *S*-parameters (S_{11} for single-polarization antenna, and S_{11} and S_{12} for dual-polarization antenna) are calculated.

Step 3: Selecting the candidate individuals for GA. For each individual in the population, its output is evaluated based on the fitness function in order to select the candidate for GA. More precisely, when the microstrip length and the

https://doi.org/10.1017/S1759078711000985 Published online by Cambridge University Press

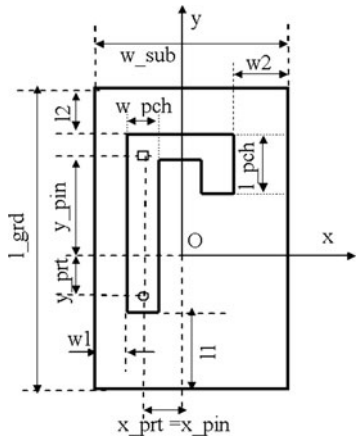

Fig. 5. L-shape microstrip patch.

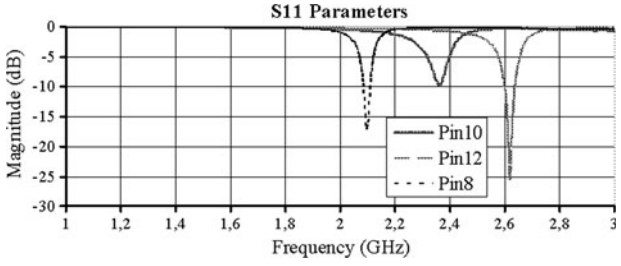

Fig. 6. Reflection coefficient, S_{11}, of the single PIFA antenna (without GA).

port value vary, only those yielding the suitable frequency band (i.e. range from 2.412 to 2.472 GHz) are considered. Then, for each value of microstrip length, the maximum value S_{11} (S_{11}_max) is sought. In the case of single polarization antenna, only pair values (microstrip length and port) with S_{11}_max < -15 dB are kept. In the case of dual-polarization antenna, only pairs with S_{11}_max < -15 dB and $S_{12} < -15$ dB are kept. The choice of candidate of shorting pin position and the air layer thickness is carried out similarly.

Step 4: Optimizing. Based on the candidates obtained from Step 3, making a crossover and mutation until the most optimal configuration possible is found.

In fact, there are iterations consisting of Steps 2, 3, and 4 for searching the best configuration (see Fig. 4).

III. SINGLE-POLARIZATION PIFA ANTENNA

The geometric parameter of the antenna is illustrated in Fig. 5. The microstrip patch has a dimension of *l_pch* × *w_pch* × *h_pch* mm^3. The thickness of the layer of air between the patch and ground plane is *h_air*. The discrete ports are located at (*x_prt*, *y_prt*) on the ground plane. The shorting is located on the dielectric substrate at (*x_pin, y_pin*). The values of those mentioned parameters are turned variable during the optimization step in order to find the best ones.

A) Simulation

In this part, we carry out several simulations of antenna with FR4 dielectric substrate having a dimension of 40 × 40 × 0.8 mm^3 in order to show the requirement of parameter optimization.

We first vary the value of *y_pin* while fixing other parameters. More precisely, *l_pch* = 10 mm, *w_pch* = 4 mm, *h_air* = 3 mm, *x_prt* = *x_pin* = −6 mm, *y_prt* = 0 mm when *y_pin* takes one of the three following values {8, 10, and 12 mm}, meaning that three antennas are considered. The reflection coefficient and the operating frequency of those antennas are, respectively, shown in Fig. 6 from which it is clear that when finding manually the position of pin which yields an optimal antenna configuration is difficult.

Similar simulations are carried out by varying *l_pch*, *h_air* and *y_prt* and fixing the rest parameters, and we observe the same problem.

Automatic parameter optimization is therefore a critical issue.

B) GA for single-polarization antenna optimizing

Table 1 presents an example of the input and output parameters when the populations are generated randomly, and Table 2 shows parameters (input and output) when fixing the length of microstrip patch (*l_pch* = 9.10 mm) and the thickness of the air layer (*h_air* = 3.0 mm), while changing the shorting pin.

As mentioned in the previous section, three antenna parameters, including the shorting pin position, the length of microstrip patch and the thickness of the air layer, are optimized simultaneously, while the port position *y_prt* is selected as one of the following values *y_prt* = {0, 1, 2, 3, and 4 mm}. For intuitiveness, the obtained values S_{11} when fixing one of three considered values while varying the others are shown in Fig. 7. There are therefore in total 3 cases: *h_air* is fixed (Fig. 7(a)), *l_pch* is fixed (Fig. 7(b)) and *y_pin* is fixed (Fig. 7(c)).

Figure 7(a) presents the results obtained when the thickness of the air layer is fixed (*h_air* = 3.0 mm). The shorting pin position takes one of the following values *y_pin* = {9.40, 9.10, 9.10, 9.05, 9.00 mm}. In this figure, the blue, green and red markers present, respectively, the S_{11} obtained with *l_pch* = 9.10, 10.10, 11.55 mm (the results represented by the blue markers correspond to those shown in Table 2 with the values S_{11} of {−19.16, −23.62, −32.23, −29.62 and −19.12 dB}).

Table 1. Parameters of the input and the output of the antenna design.

l_pch (mm)	h_air (mm)	y_prt (mm)	y_pin (mm)	F (GHz)	S_{11} (dB)
10.00	3.00	0.00	10.00	2.36	−9.83
8.95	3.00	−8.00	12.00	2.61	−25.67
6.00	3.00	−4.00	8.00	2.10	−17.19

Table 2. S_{11} parameter according to the position of the discrete port and the shorting pin.

y_prt (mm)	4	3	2	1	0
y_pin (mm)	9.40	9.10	9.10	9.05	9.00
S_{11} (dB)	−19.16	−23.62	−32.23	−29.62	−19.12

https://doi.org/10.1017/S1759078711000985 Published online by Cambridge University Press

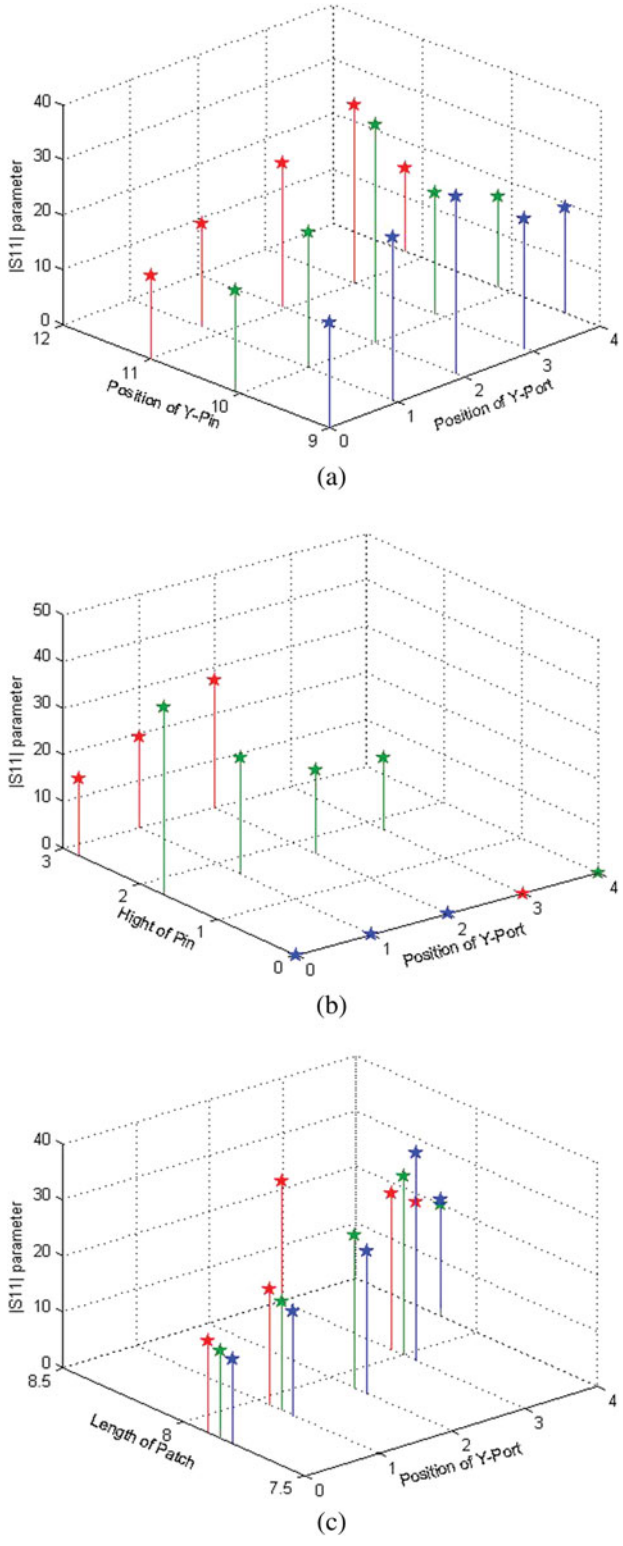

Fig. 7. Modulus of S_{11} parameter [dB]. (a) When *h_air* = 3 mm, positions of *y_pin* and *y_port* for: *l_pch* = 11.55 mm (red), 10.10 mm (green), and 9.10 mm (blue). (b) When *l_pch* = 10.10 mm, thickness of the layer of air *h_air* and position of *y_port* for: *y_pin* = 10.0 mm (red), 11.0 mm (green), and 9.0 mm (blue). (c) When *y_pin* = 10 mm, length of patch *l_pch* and position of *y_port* 2for: *h_air* = 3.0 mm (red), 2.8 mm (green), and 3.2 mm (blue).

Figure 7(b) shows the results when the length of microstrip patch equal to 10.10 mm (*l_pch* = 10.10 mm). The thickness of the air layer takes one of the following values *h_air* = (3.0, 2.8, 3.2, 2.9, and 3.1 mm). The blue, green and red markers present, respectively, the S_{11} obtained with *y_pin* = 9.0, 11.0, and 10.0 mm.

Figure 7(c) presents the results when the shorting pin position is fixed (*y_pin* = 10 mm). The length of patch takes one of the following values *l_pch* = {9.10, 10.10, and 11.55 mm}. The blue, green and red markers present, respectively, the S_{11} obtained with *h_air* = 3.0, 2.8, and 3.2 mm.

Using crossover and mutation on the samples (maximizing the value of S_{11} in this particular case), the optimal configuration is depicted in Table 3.

As computational time, with $2^{13} \times 2^{13} \times 2^{10} \times 2^{10}$ iterations, this algorithm requires a computational time of 4.5 days with a PC of 3.0 GHz, 3.25 Gb Ram and implemented on Visual Basic. It may be worth noting that the implementation on Visual Basic is about four times faster than that on Matlab.

Table 3. The parameters of the optimal antenna configuration (using GA).

Name	Value (mm)	Name	Value (mm)
l_pch	11.50	*y_prt*	−6
h_air	3.0	*x_pin*	−6
x_prt	−6	*y_pin*	11.75

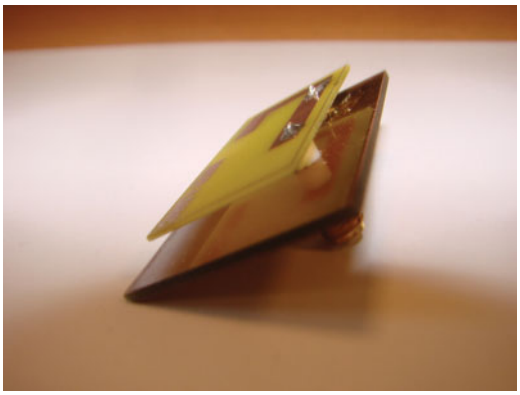

Fig. 8. Photo of the realized 2.40 GHz single-polarization PIFA antenna.

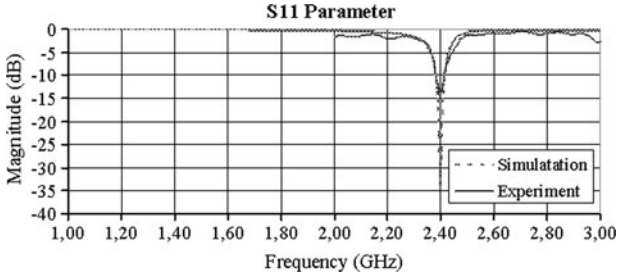

Fig. 9. Simulation and measurement results of S_{11} parameter (using GA).

C) Measurement result

The antenna is fabricated on FR4 dielectric substrate with a dimension of 40 × 40 × 0.8 mm^3. The dimension of the ground plane is 40 × 40 × 0.035 mm^3. The thickness of the

https://doi.org/10.1017/S1759078711000985 Published online by Cambridge University Press

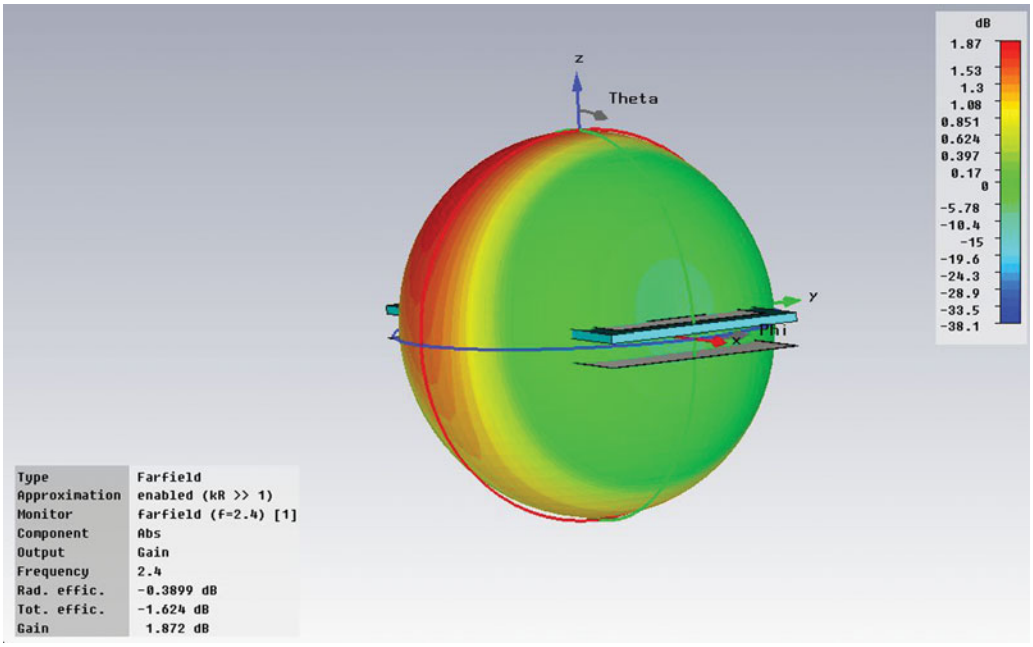

Fig. 10. Simulated radiation pattern of the single-polarization antenna.

air layer between the patch and the ground plane is 3 mm. The microstrip patch (made from Perfect Electrical Conductor (PEC)) has a dimension of $11.50 \times 4 \times 0.035$ mm^3. The discrete port is located at (−6 mm; −6 mm) and the shorting pins are located on the dielectric substrate at (−6 mm; 11.75 mm). Figure 8 shows a photo of the realized antenna.

The simulation and measurement results of the input reflection coefficient are shown in Fig. 9. The resonant frequency of the antenna is 2.43 GHz with a bandwidth equal to 300 Hz at $S_{11} = -10$ dB. When compared with the bandwidth of 400 Hz in simulation, there is a slight difference simulation and measurement results, which is due to the realization accuracy as well as the substrate, but it is clearly seen from Fig. 9 that a good agreement between simulation and measurement results is achieved.

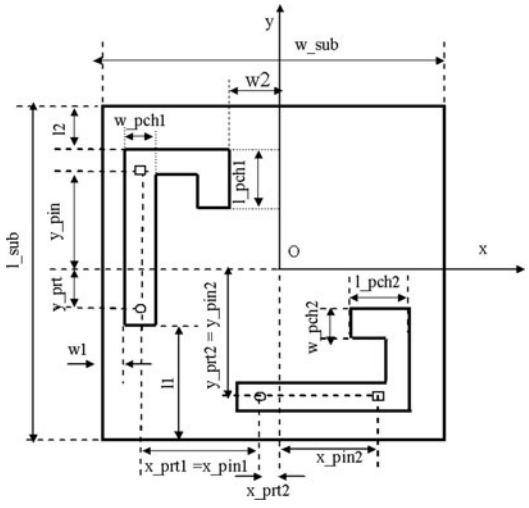

Fig. 11. Dual-polarization antenna.

Table 4. The parameters of random antenna configuration.

Name	Value (mm)	Name	Value (mm)
l_pch1	6	*x_prt2*	0
w_pch1	4	*y_prt2*	−16
l_pch2	8	*x_pin1*	−16
w_pch2	4	*y_pin1*	6
h_air	3.0	*x_pin2*	7
x_prtl	−16	*y_pin2*	−16
y_prt1	0		

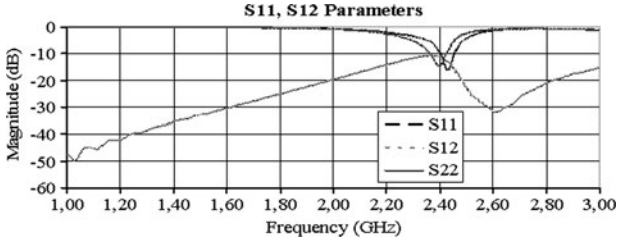

Fig. 12. S_{11}, S_{22} and S_{12} parameters of dual-polarization antenna (without GA). (a) When *h_air* = 3 mm, positions of *y_pin* and *y_port* for: *l_pch* = 9.25 mm (red), 7.75 mm (green), and 6.50 mm (blue). (b) When *y_pin* = 7 mm, thickness of the layer of air *h_air* and position of *y_port* for: *l_pch* = 7.75 mm (red), 6.50 mm (green), and 9.25 mm (blue). (c) When *l_pch* = 7.75 mm, thickness of the layer of air *h_air* and position of *y_port* for: *y_pin* = 8.0 mm (red), 7.0 mm (green), and 6.0 mm (blue).

Table 5. Parameters of the input and the output of the antenna design.

l_pchl (mm)	h_air (mm)	y_prtl (mm)	y_pinl (mm)	F (GHz)	S_{11} (dB)	S_{12} (dB)
10.00	3.00	0.00	10.00	2.8	−17.34	−25.02
8.95	3.00	−8.00	12.00	1.77	−0.28	−27.88
6.00	3.00	−4.00	8.00	2.26	−25.94	−16.11

https://doi.org/10.1017/S1759078711000985 Published online by Cambridge University Press

Table 6. S_{11} and S_{12} parameters according to the position of the discrete port and the shorting pin.

y_prt(mm)	1	0	−1	−2
y_pin (mm)	7.15	7.05	7.15	6.95
S_{11} (dB)	−15.39	−17.47	−20.50	−36.04
S_{12} (dB)	−16.95	−18.02	−18.02	−19.40

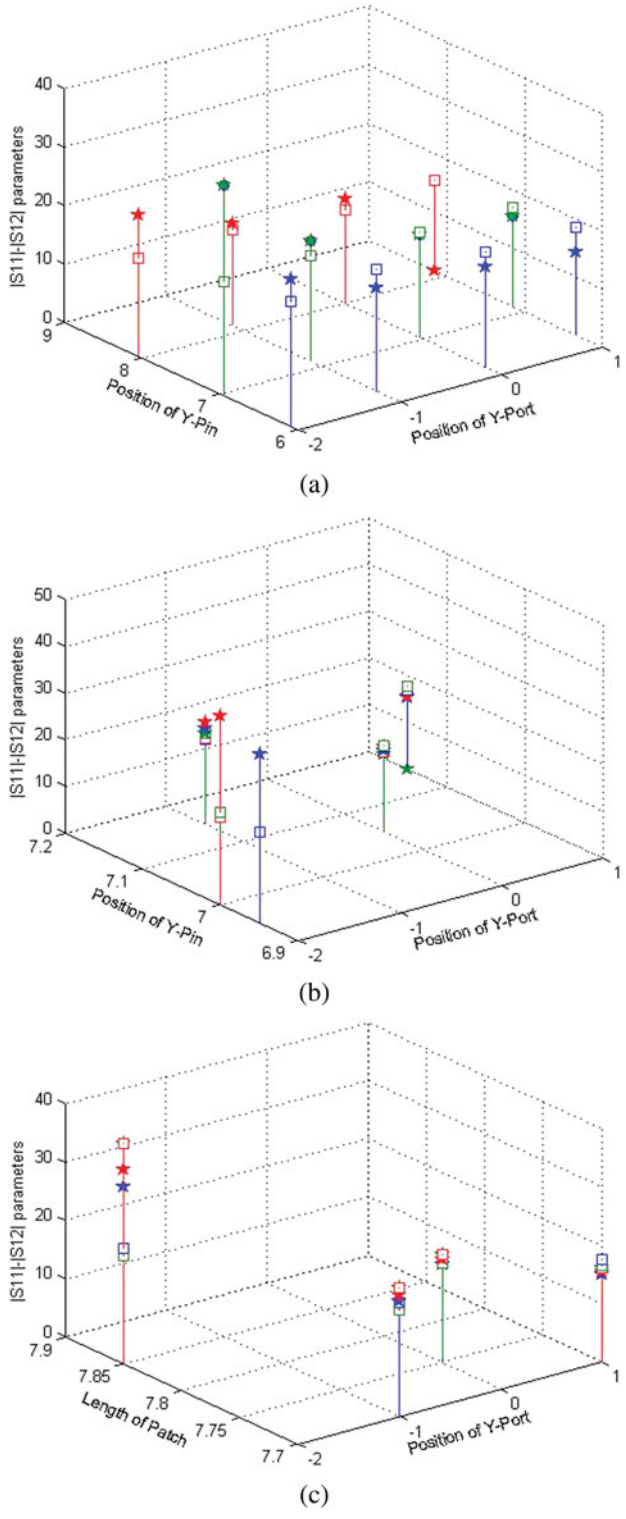

Fig. 13. Modulus of S_{11} ("star" symbol) and S_{21} ("rectangular symbol") parameters (dB).

Table 7. The parameters of the optimal antenna configuration (using GA).

Name	Value (mm)	Name	Value (mm)
l_pch1	10.25	*x_prt2*	−4
w_pch1	4	*y_prt2*	−16
l_pch2	10.25	*x_pin1*	−16
w_pch2	4	*y_pin1*	7
h_air	3	*x_pin2*	7
x_prtl	−16	*y_pin2*	−16
y_prt1	−4		

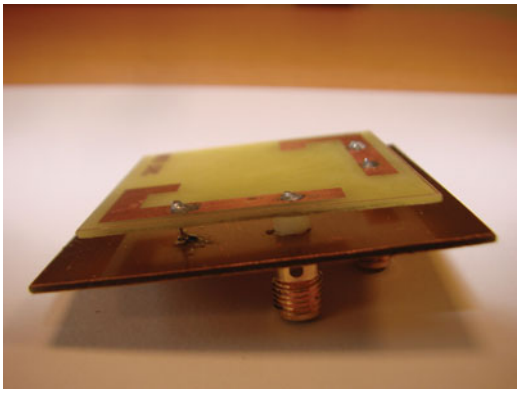

Fig. 14. Photo of the realized 2.4 GHz orthogonal polarization PIFA antenna.

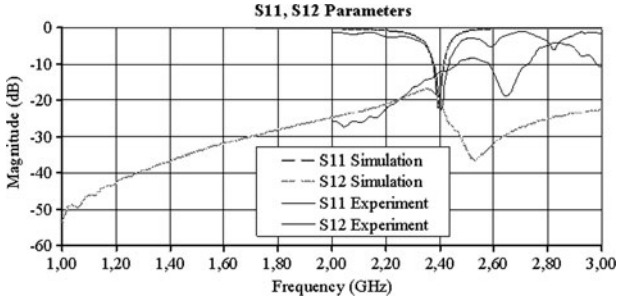

Fig. 15. Simulation and measurement results of S_{11} and S_{12} parameter (using GA). Since $S_{11} = S_{22}$, $S_{12} = S_{21}$, for clarification, only S_{11} and S_{12} are plotted here.

Finally, the 3D radiation pattern at 2.43 GHz of the single polarization PIFA is shown in Fig. 10. It can be noted that the antenna has a smooth radiation pattern such as a dipole: more precisely at 2.43 GHz the gain is 1.85 dBi.

IV. DUAL-POLARIZATION PIFA ANTENNA

The geometric antenna parameters, illustrated in Fig. 11, are: the microstrip patch with a dimension of *l_pch1* × *w_pch1* × *h_pch1* mm^3 for antenna 1 and of *l_pch2* × *w_pch2* × *h_pch2* mm^3 for antenna 2. The thickness of the air layer between the patch and ground plane is *h_air*. The discrete ports are located at (*x_prt1*, *y_prt1*) for antenna 1 and at (*x_prt2*, *y_prt2*) for antenna 2 on the ground plane. The shorting is located on the dielectric substrate at (*x_pin1*, *y_pin1*) for antenna 1 and at (*x_pin2*, *y_pin2*) for antenna 2.

https://doi.org/10.1017/S1759078711000985 Published online by Cambridge University Press

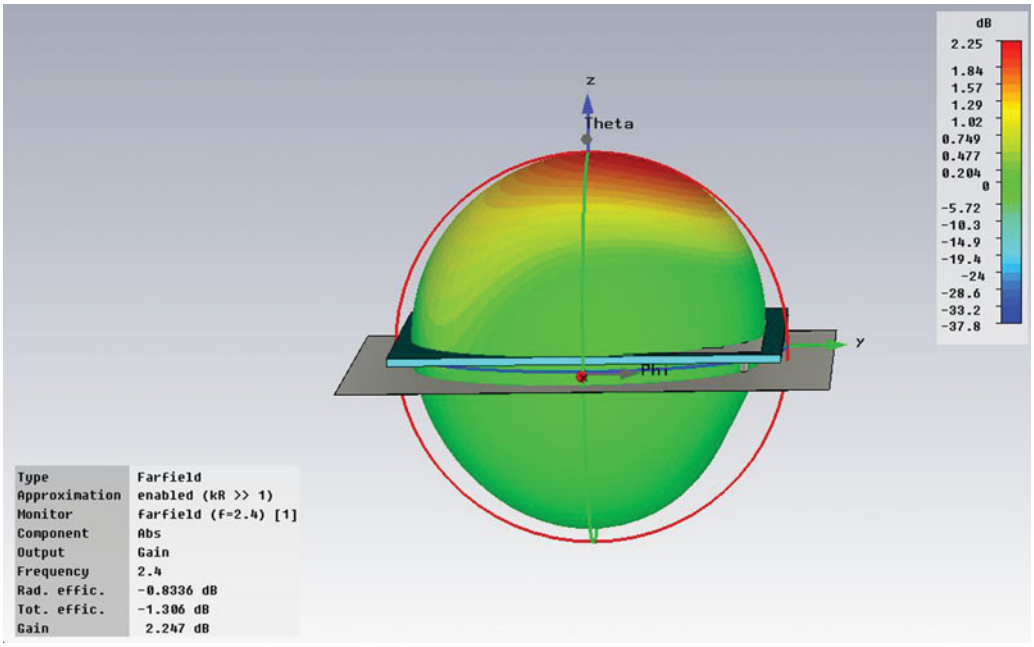

Fig. 16. Simulated radiation pattern of the dual-polarization antenna.

A) Simulation

With a configuration of antenna as shown in Table 4, the results of simulation are shown in Fig. 12. For the antenna 1, the operating frequency is 2.38 GHz and the corresponding value S_{11} is −14.83 dB. For the antenna 2, the operating frequency is 2.48 GHz and the corresponding value S_{11} is −12.66 dB.

It is clear that automatic parameter optimization is a critical issue.

B) GA for dual-polarization antenna optimizing

Table 5 presents an example of the input and output parameters when the populations are generated randomly, and Table 6 shows parameters (input and output) when fixing the length of microstrip patch ($l\_pch = 7.75$ mm) and the thickness of the air layer ($h\_air = 3.0$ mm) while changing the shorting pin.

Similar to Fig. 7, Fig. 13 proposes a synthetic and graphic presentation of the obtained results. In this figure, star markers correspond to values of S_{11}, while rectangle markers represent the values of S_{12} (Fig. 13(a) correspond to the results presented in Table 6).

Using crossover and mutation on the samples (maximizing the value of S_{11} and S_{12} in this particular case) the optimal configuration is shown in Table 7.

C) Measurement result

The antenna is fabricated on an FR4 dielectric substrate with a dimension of 40 × 40 × 0.8 mm^3. The ground plane has a dimension of 40 × 40 × 0.035 mm^3. The thickness of the air layer between the patch and the ground plane is 3 mm. The microstrip patch (made from PEC) has a dimension of 10.25 × 4 × 0.035 mm^3. The discrete port is located at (−16 mm; −4 mm) for antenna 1 and at (−4 mm; −16 mm) for antenna 2; the shorting pins are located on the dielectric substrate at (−16 mm; 7 mm) for antenna 1 and at (7 mm; −16 mm) for antenna 2. Figure 14 shows a photo of the realized antenna.

The simulation and measurement results of the input reflection and transmission coefficients are shown in Figure 15. The antenna resonant frequency is 2.43 GHz with a bandwidth equal to 500 Hz at $S_{11} = -10$ dB. It should be noted that this bandwidth is equal to 400 Hz in simulation. In fact, a small error appeared when fabricating the antenna can result in a large difference between the results of the process of simulation (the accuracy in our simulation is 0.05 mm) and that in reality. But it is clearly seen that there is a good agreement between simulation and measurement results. Consequently, we are able to confirm that the obtained parameters of the antenna with the developed GA are optimal.

Finally, Fig. 16 illustrates the radiation pattern at 2.43 GHz of the proposed PIFA antenna system. It can be clearly seen from this figure that the antenna has a smooth radiation pattern at 2.43 GHz, which is like the radiation pattern of a half-wavelength dipole with a gain of 2.15 dBi.

V. CONCLUSION

GAs are very useful for various radio electronic optimization problems, especially for optimization of antenna problem. For PIFA antenna, due to the sensitivity of the components on operating frequency and antenna efficiency, the optimization is absolutely necessary and GA is one relevant solution.

Two PIFA antennas are designed and optimized at 2.43 GHz based on GA. The GA is used to optimize antenna parameters such as operating frequency, bandwidth, and radiation pattern. The two proposed antennas are fabricated and measured. They can completely cover the required bandwidths of IEEE 802.11b/g with satisfactory radiation characteristics. The agreement of simulation and measurement results shows the performance of our joint model. The embedded GA can be further applied to other antenna configurations.

https://doi.org/10.1017/S1759078711000985 Published online by Cambridge University Press

REFERENCES

[1] Taga, T.: Analysis of planar inverted-F antennas and antenna design for portable radio equipment, in Hirasiwa, K.; Haneishi, M. (eds.), Analysis, Design and Measurement of Small and Low Profile Antenna, chapter 5, Artech House, Boston, 1992.

[2] Do-Gu, K.; Sung, Y.: Compact hexa-band PIFA antenna for mobile handset applications. IEEE Antennas Wirel. Propag. Lett., **9** (2010), 1127–1130.

[3] Chia, Z.N.C.a.M.Y.W.: Broadband Planar Antennas, John Wiley and Sons, New York, 2006.

[4] Wong, K.L.: Compact and Broadband Microstrip Antennas, John Wiley and Sons, New York, 2002.

[5] Holland, J.H.: Genetic algorithms. Sci. Am., **267** (1992), 66–72.

[6] Haupt, R.L.: An Introduction to genetic algorithms for electromagnetics. IEEE Antennas Propag. Mag., **37** (1995), 7–15.

[7] Altshuler, E.E.; Linden, D.S.: Design of a loaded monopole having hemispherical coverage using a genetic algorithm. IEEE Trans. Antennas Propag., **45** (1997), 1–4.

[8] Schlub, R.; Junwei, L.; Ohira, T.: Seven-element ground skirt monopole ESPAR antenna design from a genetic algorithm and the finite element method. IEEE Trans. Antennas Propag. **51** (2003), 3033–3039.

[9] Trong Duc, N. et al.: Optimization of PIFA antenna using an auto-embedded genetic algorithm, in Proceedings of the 3rd International Conference on Communications and Electronics (ICCE), 2010, 367–372.

[10] http://www.qls.net/va3iul/Antenna/PIFA/PIFA_Planar_Inverted_F_Antenna.pdf.

[11] http://www.cst.com/Content/Documents/Events/UGM2009/4-2-1-New-Optimization-Methods-in-CST-STUDIO-SUITE-2009.pdf.

Trong Duc Nguyen received the engineer degree and Master of Science in Information Technology from Hanoi University of Technology, Vietnam in 1998 and in 2002, respectively. From 2002 to 2008, he conducted courses and did research on Artificial Intelligence, Computer Architecture and Embedded system at the Faculty of Information Technology, Vietnam Maritime University. In 2007, he joined a research team at the Centre for Development of Advanced Computing (C-DAC), Noida, India, where his research involved embedded systems. Currently, he is a Ph.D. candidate in electronics at IMEP-LAHC laboratory, Grenoble Institute of Technology (Grenoble INP), France. His current research interests include embedded, intelligent control systems, and smart antenna systems.

Yvan Duroc received the teaching degree "Agregation" (French national degree) in Applied Physics in 1995 and the Ph.D. degree in Electrical Engineering, from the Grenoble Institute of Technology (Grenoble INP), France, in 2007. From 1997 to 2009, he worked as teaching assistant at The Engineering School Grenoble INP – ESISAR, France. Since 2009, he has been an Associate Professor of microwave and wireless systems at the Grenoble INP – ESISAR. He is in charge of lectures in applied physics, radio-frequency, signal processing, and digital communications for undergraduate and graduate students. His actual research interest concerns RF wireless systems with special attention to ultra-wideband technology and multiple antenna systems.

Van Yem Vu (associate professor) received the Ph.D. degree in communications from the Department of Electronics and Communications, TELECOM ParisTech (formerly ENST Paris) France in 2005. From 2006 to 2007, he was a postdoctoral researcher at the Department of Hyper-frequencies and Semiconductor, Institute of Electronics, Microelectronics and Nanotechnology (IEMN), France. Currently, he is the Head of the Department of Telecommunication Systems, School of Electronics and Telecommunications, Hanoi University of Science and Technology, Vietnam. Dr Vu Van Yem is also the Vice Director of the Innovation Technology Center, Hanoi University of Science and Technology, Vietnam. Dr Vu Van Yem's areas of expertise are multi-antenna communication and localization systems, microstrip antennas, and antenna array signal processing. He is member of the IEEE, REV (The Radio Electronics Association of Vietnam).

Tan Phu Vuong (senior member IEEE) was born in Vietnam. He received a Ph.D. degree in Microwaves from Toulouse Institute of Technology, France, in 1999 and HDR (Habilitation à Diriger des Recherches) degree in Microwave and Electronic from Grenoble Institute of Technology (Grenoble INP), France, in 2007. From 2001 to 2008, he was an associate professor in microwave and wireless systems at ESISAR High School of Engineer of Grenoble INP. Since 2008, he is professor at the Phelma High School of Engineer of Grenoble INP. His research interests include modeling of passive microwave and millimeter-wave-integrated circuits. His current research interests include design of small antennas and printed antennas for mobile, RFID, design of passive and active millimeter-wave components.

https://doi.org/10.1017/S1759078711000985 Published online by Cambridge University Press